

BCS - BEC crossover at $T = 0$: A Dynamical Mean Field Theory ApproachArti Garg,¹ H. R. Krishnamurthy,² and Mohit Randeria³¹Department of Theoretical Physics, Tata Institute of Fundamental Research, Mumbai 400 005, India²Centre for Condensed Matter Theory, Department of Physics,

Indian Institute of Science, Bangalore 560 012, India,

and Condensed matter Theory Unit, JNCASR, Jakkur, Bangalore 560 064, India

³Department of Theoretical Physics, Tata Institute of Fundamental Research, Mumbai 400 005, India;

Department of Physics, The Ohio State University, Columbus, OH 43210

We study the $T = 0$ crossover from the BCS superconductivity to Bose-Einstein condensation in the attractive Hubbard model within dynamical mean field theory (DMFT) in order to examine the validity of Hartree-Fock-Bogoliubov (HFB) mean field theory, usually used to describe this crossover, and to explore physics beyond it. Quantum fluctuations are incorporated using iterated perturbation theory as the DMFT impurity solver. We find that these fluctuations lead to large quantitative effects in the intermediate coupling regime leading to a reduction of both the superconducting order parameter and the energy gap relative to the HFB results. A qualitative change is found in the single-electron spectral function, which now shows incoherent spectral weight for energies larger than three times the gap, in addition to the usual Bogoliubov quasiparticle peaks.

1. INTRODUCTION

The problem of the crossover from BCS superconductivity to Bose-Einstein Condensation (BEC) of composite bosons, where the superconducting coherence length (roughly the size of the fermion pair binding) is respectively much larger than or much smaller than the average inter-fermion spacing, has been a problem of great interest from the very early stages of development of the theory of superconductivity. It was first addressed in the very early work of Eagles [1]. In 1980 Leggett [2] showed, using a variational approach, that at zero temperature the superconducting BCS ground state at weak coupling evolves smoothly into a Bose condensate state of tightly bound "molecules" at strong coupling. Nozieres and Schmitt-Rink [3] extended the analysis to lattice models and to finite temperature and showed that the transition temperature T_c between the normal and the superconducting state evolves continuously as a function of the magnitude of the attractive interaction between the fermions. The discovery of high T_c superconductors, which are characterized by short coherence length comparable to (but larger than) the inter-particle spacing, led to a resurgence of interest in the BCS-BEC crossover. A variety of interpolation schemes between weak and strong coupling developed using variational methods, functional integrals, and diagrammatic methods have been explored [4, 5, 6], and the existence of pseudo-gap anomalies in the normal state of a short coherence length superconductor has been established in two-dimensional systems [7, 8]. Recently it has become possible to directly realize the BCS-BEC crossover in a dilute atomic gas of Fermi ions in a trap, by varying their two-body interaction (scattering length) using a Feshbach resonance [9].

In this paper we analyze the BCS-BEC crossover in the attractive Hubbard model using the dynamical mean

field theory (DMFT) [10, 11] approach. Our goal is to focus on the intermediate coupling regime $U=t$ where one has no obvious small parameter. Since the DMFT becomes exact in the limit of infinite dimensions [10, 11], we are, in a sense, using the inverse coordination number of the lattice as the small parameter. The attractive Hubbard model has been studied recently using DMFT, but primarily in the normal phase [12] to analyze pair formation above T_c and related phenomena. We focus here on the superconducting phase at zero temperature, in part because the DMFT method has been much less explored in broken symmetry phases.

The remainder of the paper is organized as follows. In Section 2, we define the model and review the Hartree-Fock-Bogoliubov (HFB) mean field theory. In Section 3, we briefly summarize the DMFT approach in the superconducting (SC) state and then describe the specific implementation of DMFT which we use, namely the iterated perturbation theory (IPT), in Section 4. In Section 5 we present our results for the chemical potential, energy gap, SC order parameter, density of states, spectral function, occupation probability and superfluidity. We discuss how each of these evolves from the weak coupling BCS limit to the strong coupling BEC limit, and to what extent the quantum fluctuations included in the DMFT implemented using IPT modify the results relative to HFB mean field theory.

2. MODEL

We use the simplest lattice model which exhibits the BCS-BEC crossover, defined by the Hamiltonian

$$H = \sum_{ij} t c_i^\dagger c_j + \sum_i \frac{U n_i n_{i\#}}{2} - \sum_i \epsilon_i n_i \quad (1)$$

The first term describes the kinetic energy of fermions with nearest neighbor hopping t , the on-site attractive interaction (U) induces s-wave, singlet pairing and leads to a superconducting ground state for all $n \neq 1$, with the chemical potential determining the filling factor n . We will not study the system with $n = 1$ for which superconducting and charge-density wave orders coexist.

The simplest mean-field description of this system uses the Hartree-Fock-Bogoliubov (HFB) theory leading to the following self-consistent equations for the "gap" and at a temperature $T = 1/(k_B)$:

$$\frac{1}{U} = \frac{X}{k} \frac{\tanh(E_k/2)}{2E_k} \quad (2)$$

and

$$n = \frac{X}{k} = 1 - \frac{k}{E_k} \tanh \frac{E_k}{2} \quad : \quad (3)$$

We use standard notation where p is the band dispersion for the fermions and $E_k = \sqrt{\frac{p^2}{2} + \frac{t^2}{k^2}}$ with k $\propto \sqrt{U}$. As is well known [4, 5, 6, 13] at $T = 0$ the solution of these equations leads to a BCS superconductor in the weak coupling $U/t \ll 1$ limit, to a BEC of hard core bosons in the opposite extreme $U/t \gg 1$, and interpolates smoothly in between. However, the finite temperature solutions of these equations for $U/t \ll 1$ yields a $T_c \propto U$ not the BEC transition temperature scale expected to be of order $t^2 = U/t$ and the HFB approach therefore does not constitute an interpolating approximation at finite T [4].

The DMFT is one of the simplest schemes that has the potential to overcome some of these limitations of simple HFB theory. As we discuss in the following sections, the lattice dependence of quantities that arise in the DMFT is not via the momentum k but only via the band dispersion k , and hence we can make the replacement

$$\frac{X}{k} = \frac{Z}{k} \frac{1}{d(\epsilon)} \quad (4)$$

where (ϵ) is the (bare) band density of states (DOS). The implementation of the DMFT is often simplest on a Bethe lattice with a large coordination number $z = 1$, for which

$$d(\epsilon) = \frac{p}{2t^2} \frac{4t^2 - \epsilon^2}{(2t - \epsilon)^2} \quad (5)$$

if the bare hopping is normalized as

$$t = \frac{p}{z} \quad (6)$$

We conclude this section by calculating the effective two-body interaction or the low energy scattering amplitude, which should also help to clarify the connection between the continuum Fermi gases often studied

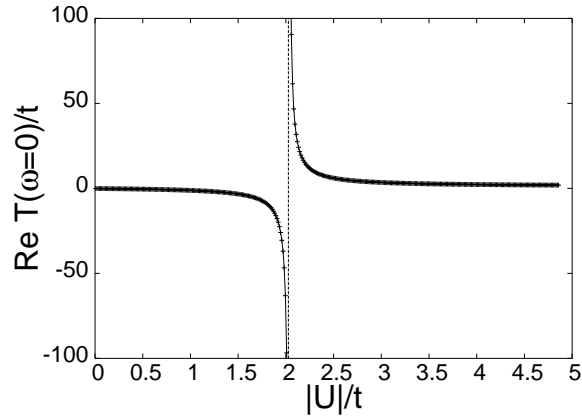


FIG. 1: The real part of the transmission $T(\omega = 0)$ for the two-body problem is plotted as a function of the attraction U/t between two fermions in an otherwise empty Bethe lattice of infinite connectivity. $U/t = 2$ is the threshold for the formation of bound state in vacuum.

theoretically (and now experimentally) and the lattice model studied in this paper. The low energy scattering amplitude is given by the real part of the transmission $Re T(\omega = 0)$ for the two-body problem in vacuum, i.e., for two fermions in an otherwise empty lattice. This is the analog of the well known three-dimensional "scattering length" for the case of the Bethe lattice studied in this paper. As shown in Fig. 1, for $U/t < 2$ the interaction is attractive but not sufficient to cause a two-body bound state, and $U/t = 2$ is the threshold for bound state formation at which the scattering amplitude diverges [14].

3. DYNAMICAL MEAN FIELD THEORY

To explore the intermediate coupling regime we use the dynamical mean-field theory (DMFT) approach [10, 11], which reduces a lattice problem with many degrees of freedom to an effective single-site problem by "integrating out" all the fermionic degrees of freedom except those at one site (the "impurity site") and retaining the effects of this only in the form of a self-consistently determined bath with which the "impurity site" hybridizes. This retains non-trivial local quantum fluctuations missing in conventional mean-field theories and the description can be shown to be exact in the limit of large dimensionality. Since there are many excellent reviews of DMFT we will only outline the elements of the technique in order to introduce our notation and to indicate the changes in the standard formalism necessitated by the presence of the superconducting long range order.

To take the superconducting order (with singlet pairing) into account we use the Nambu formalism with the spinors $\begin{pmatrix} \psi_k \\ \psi_{-k}^* \end{pmatrix}$ and the matrix Green's function

$$\hat{G}(k; \omega) = i\Gamma(k; \omega) - \psi(k; 0)i$$

$$= \begin{pmatrix} G(k; \cdot) & F(k; \cdot) \\ F^Y(k; \cdot) & G(-k; \cdot) \end{pmatrix} \quad (7)$$

where $F(k; \cdot) = \text{hT} \alpha_k(\cdot) \text{c}_{k\#}(0)$ satisfies $F(-k; \cdot) = F(k; \cdot)$. We will denote all Nambu matrices by a 'hat' on top. In this formalism the interaction effects are described in terms of the self energy matrix

$$\hat{\alpha}(k; i!_n) = \begin{pmatrix} (k; i!_n) & S(k; i!_n) \\ S^2(k; i!_n) & ?(k; i!_n) \end{pmatrix} \quad (8)$$

where $i!_n = (2n + 1)$ are fermionic Matsubara frequencies.

In the limit of infinite dimensions it can be shown that the self energy is purely local, i.e., is k independent (see ref. 10), so that $\hat{\alpha} = \hat{\alpha}(i!_n)$. Furthermore, the SC order parameter can be chosen to be real in a uniform system, which implies that $S(i!_n) = S^2(i!_n)$. Hence using the Dyson equation the full Green's function for the lattice can be written as

$$\hat{G}^{-1}(k; i!_n) = \begin{pmatrix} i!_n + & k & 0 & \hat{\alpha}(i!_n) \\ 0 & i!_n & +_k & \end{pmatrix} \quad (9)$$

$$= \begin{pmatrix} i!_n + & k & (i!_n) & S(i!_n) \\ S(i!_n) & i!_n & +_k + (-i!_n) & \end{pmatrix}$$

Thus, in DMFT the k -dependence in $\hat{G}^{-1}(k; i!_n)$ enters only via the dispersion k .

The local self energy is itself obtained from an effective single site problem which can be regarded as arising from integrating out fermionic variables on all sites except one. The effective action for this single site problem within the DMFT approximation is given by

$$S_{\text{eff}} = \begin{pmatrix} Z & Z \\ 0 & 0 \end{pmatrix} \begin{pmatrix} d^0 & Y(\cdot) \hat{G}^{-1}(\cdot, 0) & 0 \\ 0 & \hat{G}^{-1}(0, \cdot) & Z \\ \int j_0 d n_{\#}(\cdot) n_{\#}(\cdot) & 0 & \end{pmatrix} \quad (10)$$

Here the host (M)atrix Green's function \hat{G} is not the non-interacting local Green's function, as it includes the effects of the fermionic degrees of freedom at other sites which have been integrated out in the presence of interactions, i.e., it includes (local) self energy corrections at all these other sites, and needs to be determined by a triangle of self-consistency relations as described below.

The first of these relations comes from the requirement that the "impurity" Green's function for the single site problem should be the same as the local Green's function of the lattice, so that

$$\hat{G}(i!_n) = \sum_k \hat{G}(k; i!_n) \quad (11)$$

This gives the diagonal and off-diagonal components of the impurity Green's function as

$$G(i!_n) = \begin{pmatrix} Z_1 & 1 \\ 1 & \end{pmatrix} \frac{1}{(x_1)(x_2) + S^2(i!_n)}; \quad (12)$$

and

$$F(i!_n) = S(i!_n) \begin{pmatrix} Z_1 & 1 \\ 1 & \end{pmatrix} \frac{1}{(x_1)(x_2) + S^2(i!_n)} \quad (13)$$

Here $x_1 = i!_n + \hat{\alpha}(i!_n)$ and $x_2 = i!_n + +(-i!_n)$. For the case of the semi-circular DOS of eq. (5) the integrals can be evaluated in closed form as

$$G(i!_n) = \frac{2}{x_1 - x_2} \frac{1}{x_1 + \frac{p}{x_1^2 - 4\ell^2}} \frac{1}{x_2 + \frac{p}{x_2^2 - 4\ell^2}} \quad (14)$$

$$F(i!_n) = \frac{S(i!_n)}{x_1 - x_2} \frac{1}{x_1 + \frac{p}{x_1^2 - 4\ell^2}} \frac{1}{x_2 + \frac{p}{x_2^2 - 4\ell^2}} \quad (15)$$

with $x_{1,2} = \frac{1}{2} \sqrt{(\ell^2 + i!_n)^2 - 4S^2(i!_n)} = 2$.

The second relation comes from the Dyson equation connecting the full Green's function \hat{G} at the impurity site, the host Green's function \hat{G} and the self-energy $\hat{\alpha}$, typically used in reverse, in the form

$$\hat{G}^{-1}(i!_n) = \hat{G}^{-1}(i!_n) + \hat{\alpha}(i!_n); \quad (16)$$

The final relation comes from the solution for the self energy of the impurity problem defined by (10), i.e., the determination of

$$\hat{\alpha}(i!_n) = \hat{\alpha}[\hat{G}(i!_n)] \quad (17)$$

from a knowledge of the host Green's function. This is the task of the "impurity solver", and is typically the hardest step in the triangle of self consistency. In this paper, we use iterated perturbation theory (suitably extended to deal with the broken symmetry associated with the superconducting ground state as described in the following section) as the impurity solver.

4. ITERATED PERTURBATION THEORY

We adapt the iterated perturbation theory (IPT), originally developed for the paramagnetic phase of the repulsive Hubbard model [10, 15], to the SC phase of the attractive Hubbard model. IPT is an approximate technique which is much simpler than the more accurate but elaborate alternate methods such as quantum Monte Carlo [16], exact diagonalization [17], numerical renormalization group [18], local moment approximation [19] etc. IPT gives semi-analytical results which can be directly and easily continued to the real frequency domain.

In the form in which we use it here [20], it rests on the following ansatz for the self energy as a functional of \hat{G} :

$$\hat{\Sigma}_{\text{IP T}}(\omega) = \hat{\Sigma}_{\text{HFB}} + \hat{A}^{(2)}(\omega) : \quad (18)$$

Here $\hat{\Sigma}_{\text{HFB}}$ is the Hartree-Fock-Bogoliubov (HFB) self energy as in eq. 19 (see note [21]), $\hat{\Sigma}^{(2)}$ is the second order perturbation theory result (in powers of μj) but calculated in terms of the Hartree-corrected host Green's function (see eq. 24), and \hat{A} is to be determined as described below (see eq. 28). All the calculations we report and discuss in this paper are done at $T = 0$, and we work directly in real frequency $\omega = \omega + i0^+$.

The IPT ansatz is constructed so that [20] it

reproduces the leading order terms for the self energy in the weak coupling limit $\mu j \ll t$,

is exact in the atomic limit $t = \mu j = 0$, and

reproduces the leading order terms for the self energy in the large t limit for all $\mu j \gg t$, which ensures that some exact sum rules are satisfied.

Thus IPT is expected to provide a reasonable interpolating scheme between the weak and strong coupling limits.

The HFB self energy is given by

$$\hat{\Sigma}_{\text{HFB}} = \mu j \frac{n}{2} \hat{\Sigma}_z \quad \hat{\Sigma}_x \quad (19)$$

Here $\hat{\Sigma}_z$ and $\hat{\Sigma}_x$ are Pauli matrices in Nambu space. The filling factor $n = \frac{1}{2} \text{Im } G(\omega=0)$ and $\mu j = \mu j c_s c_a$, with c_s being the superconducting order parameter, are obtained from the full Green's function within IPT as

$$n = \frac{1}{2} \sum_{\alpha} \text{Im } G(\omega=0) d\alpha \quad (20)$$

$$= \frac{\mu j}{2} \sum_{\alpha} \text{Im } F(\omega=0) d\alpha \quad (21)$$

The diagonal and off-diagonal components of the second order self energy $\hat{\Sigma}^{(2)}$ are given by

$$\hat{\Sigma}^{(2)}(t) = U^2 G_{11}(t) G_{22}(-t) G_{22}^Y(t) F_0^Y(t) G_{22}(-t) F_0(t) \quad (22)$$

and

$$S^{(2)}(t) = U^2 F_0(t) F_0(-t) F_0^Y(t) G_{11}(t) F_0(-t) G_{22}(t) \quad (23)$$

Here G_{11} , G_{22} , F_0^Y and F_0 are components of the Hartree-corrected Host Green's function matrix

$$\begin{aligned} G_{11}(\omega) F_0(\omega) &= G_0(\omega) F_0(\omega) & \hat{\Sigma}_{\text{HFB}} \\ F_0^Y(\omega) G_{22}(\omega) &= F_0(\omega) G_0^2(\omega) \end{aligned} \quad (24)$$

The subscript 0 has been added in order to distinguish the components of the host green functions that arise

in the specific context of the IPT approximation to the impurity problem.

Each of the terms in (22) and (23) is the product of three factors of the form

$$H(t) = h_1(t) h_2(-t) h_3(t) \quad (25)$$

where each h_i is either G_{11} , G_{22} , F_0^Y or F_0 . Using the spectral representation for each Green's function we obtain for the Fourier transform,

$$H(\omega) = \sum_{i=1}^{Z/2} \frac{Y^3}{d_i \gamma_i(\omega)} \frac{N(\omega_1; \omega_2; \omega_3)}{\omega_1 + \omega_2 + \omega_3} \quad (26)$$

where $\gamma_i(\omega) = \text{Im } h_i(\omega)$ and $N(\omega_1; \omega_2; \omega_3)$ is a thermal factor

$$N(\omega_1; \omega_2; \omega_3) = f(\omega_1) f(\omega_2) f(\omega_3) + f(-\omega_1) f(-\omega_2) f(-\omega_3) \quad (27)$$

involving the Fermi function $f(\omega) = 1/(1 + \exp(\omega/\mu)) = 1 - f(-\omega)$.

The matrix \hat{A} in (18) is fixed by demanding that $\hat{\Sigma}_{\text{IP T}}(\omega)$ is "exact" in the large t limit up to order $1/t$. As shown in Appendix A, we find \hat{A} to be proportional to the identity matrix $\hat{\Sigma}_0$ in Nambu space and given by

$$\hat{A} = \frac{U^2 n_0}{2} \begin{pmatrix} 1 & \frac{n_0}{2} & \frac{1}{2} & \frac{U^2 n}{2} & 1 & \frac{n}{2} & \frac{1}{2} & \hat{\Sigma}_0 \end{pmatrix} \quad (28)$$

where $\hat{\Sigma}_0$ is the identity matrix. Here n_0 and μj_0 denote "filling factor" and "gap function" values evaluated for the Hartree-corrected Host Green's function, i.e.,

$$n_0 = \frac{1}{2} \sum_{\alpha} \text{Im } G_{11}(\omega=0) d\alpha \quad (29)$$

and

$$\mu j_0 = \frac{1}{2} \sum_{\alpha} \text{Im } F_0(\omega=0) d\alpha : \quad (30)$$

In the atomic limit, as discussed in Appendix B, we find that the second order self energy vanishes. Thus the IPT self energy for $t=U=0$ is simply the HFB self energy. We show in Appendix B that the HFB result is exact at zero temperature in the broken symmetry phase for $t=U=0$, and thus our ansatz for the self energy is exact in the atomic limit.

5. RESULTS

We have solved the DMFT equations within the IPT approximation as follows. For a given μj and n , we start with a guess for the self energy $\hat{\Sigma}(\omega)$ and the chemical potential μ . With this self energy as input,

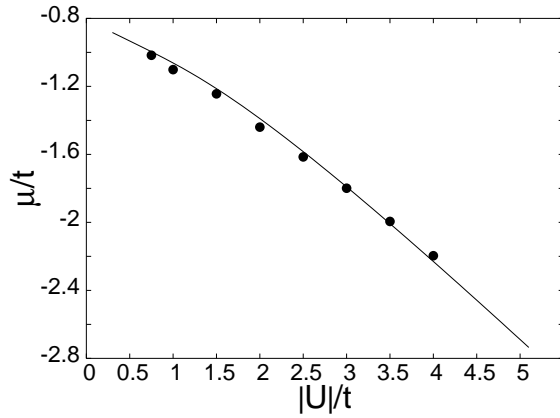


FIG. 2: The chemical potential u/t as a function of $|U|/t$ for $n = 0.5$ and $T = 0$ within IPT (filled circles) and HFB theory (full line).

we compute the full local Green's function $\hat{G}(!^+)$ using analytically continued form of eqs. (14) and (15) at $T = 0$. Then we use the Dyson equation (16) to determine the host Green's function \hat{G} . Next we use the IPT ansatz (18-24) to determine the (new) self energy in terms of \hat{G} , using new values of parameters ϵ_0 and n_0 . Finally we obtain the new chemical potential by solving the filling constraint equation (20) using the Royden method [22]. We then iterate the whole procedure until a self-consistent solution is reached, i.e., convergence in the self energy matrix is achieved.

Within this self-consistency loop the evaluation of n and n_0 using eq. (20) and (21) (and similarly for n_0 and ϵ_0) involves integrals with singular integrands: the functions $\text{Im } G(!^+)$ and $\text{Im } F(!^+)$ have square root singularity at a gap edge $\epsilon = E_g$ which is not a priori known. We fit these functions in a small neighborhood of the gap edge to the form $K = \frac{1}{\epsilon - E_g}$, where the K s determine the gap in the spectrum E_g . Then the singular part of integral near the gap edge is easily evaluated analytically and the part away from the singularity evaluated numerically using Gaussian quadrature.

All of the results reported in this paper have been obtained at a fixed density of $n = 0.5$ (quarter filling) in order to avoid special features that arise at half-filling. (At half-filling, corresponding to $n = 1$, charge density wave order becomes degenerate with SC order and the Hamiltonian has $SU(2)$ symmetry, and is in fact isomorphic to the repulsive Hubbard model which has been well-studied within DMFT.) We expect similar results for $n \neq 1$.

Chemical potential: Fig. 2 shows the chemical potential tuned to obtain $n = 0.5$ at $T = 0$. We see that it decreases monotonically as a function of $|U|/t$ and the system becomes non-degenerate with increasing attraction between the fermions. For $|U|/t > 3.5t$ the chemical potential goes below the bottom of the band.

Density of states: The single particle density of

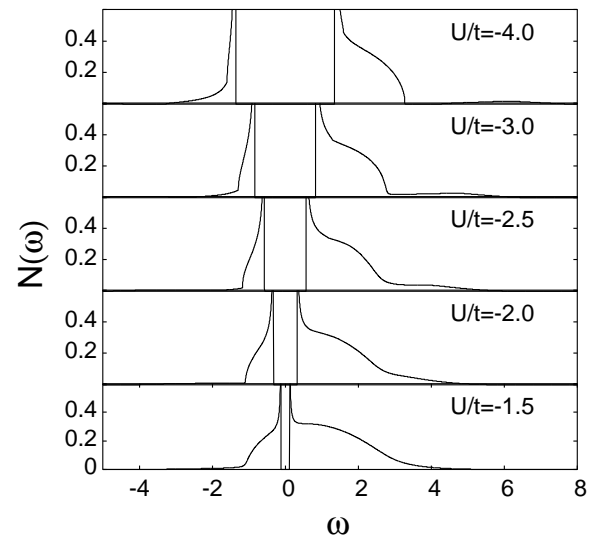


FIG. 3: Single particle density of states (per unit energy per unit area) for $n = 0.5$ and $T = 0$ within IPT for Bethe lattice of infinite connectivity.

states (DOS) $N(!)$

$$N(!) = -\frac{1}{\pi} \text{Im } G(!^+) \quad (31)$$

is plotted in Fig. 3 for various values of $|U|/t$. We observe a spectral gap (E_g) in the single particle DOS, which increases with $|U|/t$ as shown in Fig. 4, where the gap as obtained within the HFB theory is also shown for comparison.

For weak coupling the HFB spectral gap has the form $\text{exp}(-t=2|U|)$, characteristic of BCS theory, while for large attraction it approaches to the binding energy of the composite bosons being proportional to $|U|/2$. The differences of the DMFT result for the energy gap from the simple HFB estimates will be discussed below. Near the gap edge the DOS has a square root singularity characteristic of a s -wave superconductor. But the DOS far from the gap edge does not simply look like the non-interacting semi-circular DOS of the Bethe lattice (as would be the case in weak coupling BCS theory). The structure at larger energy values comes from the $!$ dependence of the self energy, as we discuss below.

Order parameter and energy gap: The superconducting order parameter is calculated using

$$Z_0 = \hbar c \sigma_i = 1 = \frac{1}{\pi} \text{Im } F(!^+) d!$$

and plotted in Fig. 5. We see that, as expected, the quantum fluctuations included in DMFT suppress the order parameter below its HFB mean-field value. The effect of quantum fluctuations in the intermediate coupling regime can be seen more clearly in Fig. 6 where we plot the fractional deviation of DMFT order parameter

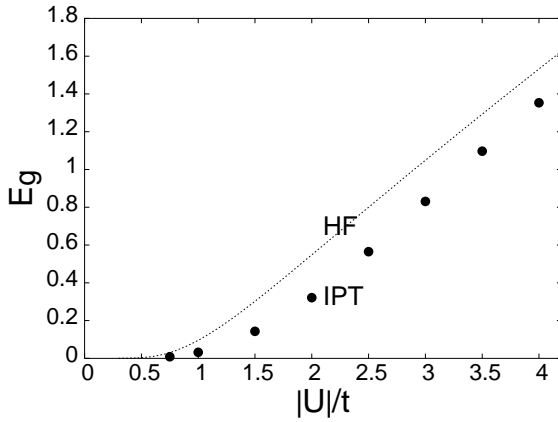


FIG. 4: The spectral gap in the single particle density of states for $n = 0.5$ and $T = 0$ as a function of $|U|/t$ within IPT (filled circles) and HFB theory (dotted line). Note that the spectral gap within IPT is suppressed as compared to that obtained from HFB theory.

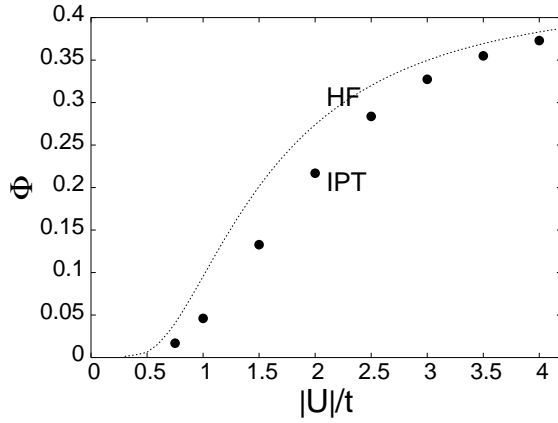


FIG. 5: The superconducting order parameter for $n = 0.5$ and $T = 0$ within IPT (filled circles) and HFB theory (dotted line). Note that the order parameter within IPT is suppressed as compared to that obtained from HFB theory.

and the energy gap from their corresponding HFB values. For small to intermediate values of the coupling $U < t$ the quantitative differences are quite large with the HFB results being larger than the DMFT ones by more than 100%.

Spectral function :

Another important quantity of interest is the one-particle spectral function

$$A(\omega; \epsilon) = -\frac{1}{\pi} \text{Im} G(\omega; \epsilon^+) \quad (32)$$

where G is the "11" component of the Nambu Matrix Green's function for the lattice obtained by inverting eqn. 9, and is given by

$$G(\omega; \epsilon^+) = \frac{\omega + \epsilon^+ - (\epsilon^+)^+}{D(\omega; \epsilon^+)} \quad (33)$$

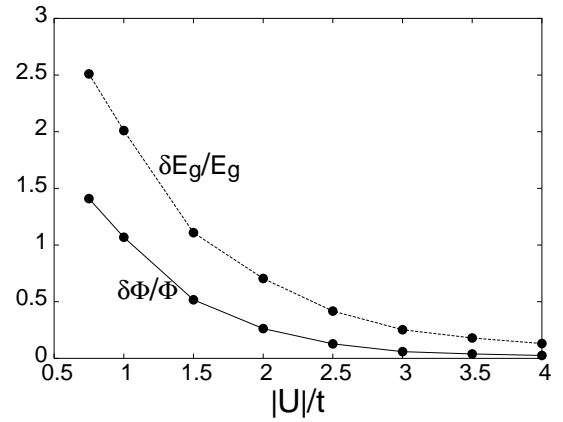


FIG. 6: $\delta E_g/E_g$ where E_g is the SC order parameter within HFB theory and E_g is the same within IPT. $E_g = E_g$ where E_g is the spectral gap within HFB theory and E_g is the same within IPT.

with

$$D(\omega; \epsilon) = \omega + \epsilon^+ - (\epsilon^+)^+ \quad (34)$$

$$+ \omega + (\epsilon^+)^+ - \epsilon^+ + (\epsilon^+)^+ - S^2(\epsilon^+)$$

Since we are working within the DMFT framework, we have traded the k label for the energy label.

Quite generally, we expect that the spectral function will be of the form

$$A(\omega; \epsilon) = Z_+(\omega - E) + Z_-(\omega + E) + A_{\text{inc}}(\omega; \epsilon) \quad (35)$$

where $Z_+(\omega)$ are the coherent spectral weights in the Bogoliubov quasiparticle/quasihole excitation poles at energies $E(\omega)$, and A_{inc} is the incoherent part of the spectral function. We recall that in simple BCS-HFB mean field theory $Z_+ = (1 - \omega/E)^{-1/2}$ where $\omega = \sqrt{2|U|j^2}$ and $E = \sqrt{\omega^2 + \epsilon^2}$ and $A_{\text{inc}} = 0$. In contrast, as shown in Fig. 7 the DMFT result for $A(\omega; \epsilon)$ not only has sharp delta function peaks at E corresponding to the Bogoliubov excitations but also has a broad incoherent part. The weight in the coherent excitations $Z_+ + Z_- < 1$ and the deficit from unity is contained in A_{inc} . All of this is a consequence of the frequency dependent self-energy as shown below.

The imaginary part of the (diagonal) self-energy is plotted in Fig. 8. It vanishes at low energies ($|\epsilon| < 3E_g$) since there are no final states available for a scattering event. In this regime, from eqs. (32) and (33) it follows that

$$A(\omega; \epsilon) = (\epsilon^+ - \omega) D(\omega; \epsilon^+); \quad (36)$$

with $D(\omega; \epsilon) = (\epsilon^+ - \omega) (\epsilon^+ + \omega) (\epsilon^+ + S^2(\epsilon^+))$, since ϵ^+ and $S^2(\epsilon^+)$ are now real. The quasiparticle excitation energies are the two symmetrically placed

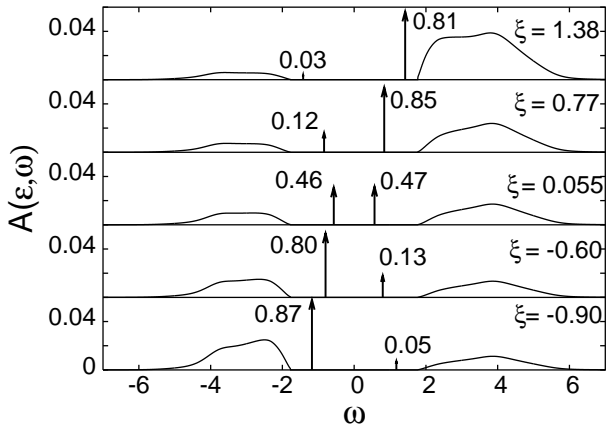


FIG. 7: The spectral function $A(\epsilon; \omega)$ for $n = 0.5$, $T = 0$ and $\hbar j = 2.5t$ as a function of ω for various values of $\xi = \epsilon - E_g$. Note that $A(\epsilon; \omega)$ not only has coherent delta function peaks (which are shown by arrows with the corresponding weights) but also has broad incoherent parts which start appearing for $\omega \gtrsim 3E_g$. For $\hbar j = 2.5t$, $E_g = 0.57t$.

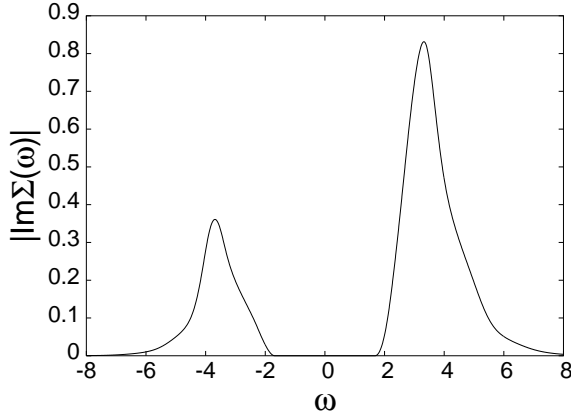


FIG. 8: The imaginary part of self-energy $\text{Im}\Sigma(\omega)$ for $n = 0.5$, $T = 0$ and $\hbar j = 2.5$ as a function of ω . Note that $\text{Im}\Sigma(\omega)$ becomes non-zero only for $\omega \gtrsim 3E_g$. For $\hbar j = 2.5t$, $E_g = 0.57t$.

zeros at $\omega = E$ of D which is an even function of ω . Thus the excitation energies are given by

$$D(\omega; E) = 0; \quad (37)$$

and the residues at the Bogoliubov quasiparticle poles are then reduced compared to their HFB values and are given by

$$Z(\omega) = [E + \text{Im}\Sigma(\omega) - E] \frac{\partial D}{\partial \omega} (\omega = E) \quad (38)$$

The imaginary part of the (diagonal) self energy becomes non-zero for $\omega \gtrsim 3E_g$, since in that case there are final states available for scattering, say, an injected particle or a particle-hole pair; see Fig. 8. This leads to the incoherent part of the spectral function $A_{\text{inc}}(\omega; \omega)$. The

reduction of the coherent quasiparticle weight and the transfer of spectral weight to the incoherent part of the spectral function are thus features related to the ω dependent selfenergy and are missing in simple HFB mean field theory.

Occupation probability: We next calculate the analog of the momentum distribution within the DMFT, namely the occupation probability $n(\omega)$ of an energy level given by

$$n(\omega) = \frac{Z_0}{Z_1} A(\omega; \omega) \quad (39)$$

This is plotted in Fig. 9 for various values of $\hbar j t$.

Within the HFB approximation, $n(\omega)$ has the following simple form :

$$n(\omega) = Z(\omega) = \frac{1}{2} \frac{1}{1 - \frac{\omega}{E}} \quad (40)$$

It is easy to see that in the weak coupling limit $n(\omega)$ looks like a slightly broadened Fermi function, dropping from 1 to zero over an energy scale of order E ; its width hence increases monotonically with $\hbar j t$. As one begins to form more and more tightly bound pairs, higher states need to be involved in the pairing and eventually the system becomes non-degenerate even at $T = 0$ as already argued from the chemical potential. Note that $n(\omega)$ within IPT is always less rounded than that within HFB because quantum fluctuations reduce the gap in the single particle dos relative to HFB value.

We find that the exact sum rule $\int_{-\infty}^{\infty} n(\omega) d\omega = n=2$ is satisfied in our IPT calculation within the estimated numerical errors (0.4% – 2%).

Superuidity: We can also estimate an upper bound on the superuidity D_s which is the strength of the delta function in the real part of optical conductivity :

$$\text{Re}(\omega) = D_s(\omega) + \text{Re}_{\text{reg}}(\omega); \quad (41)$$

The Kubo formula for the superuidity [23] can be written as

$$\frac{D_s}{\omega} = \hbar K_x i \text{Re}_T(q_x = 0; q_y = 0; \omega = 0) \quad (42)$$

where the kinetic energy $\hbar K_x i$ is the diamagnetic response of the system to the vector potential and the transverse current-current correlation function T is the paramagnetic response. It is easy to see that $T = 0$, so that $D_s = \hbar K_x i j$. Thus the kinetic energy gives an upper bound to the superuidity, and in fact we may use it to provide a rough estimate of D_s (although, as emphasized in ref. [24], there is no reason to assume in general that for a lattice model D_s is identical to $\hbar K_x i j$ even though this equality holds within simple BCS-HFB theory.) In Fig. 10 we plot the superuidity D_s as

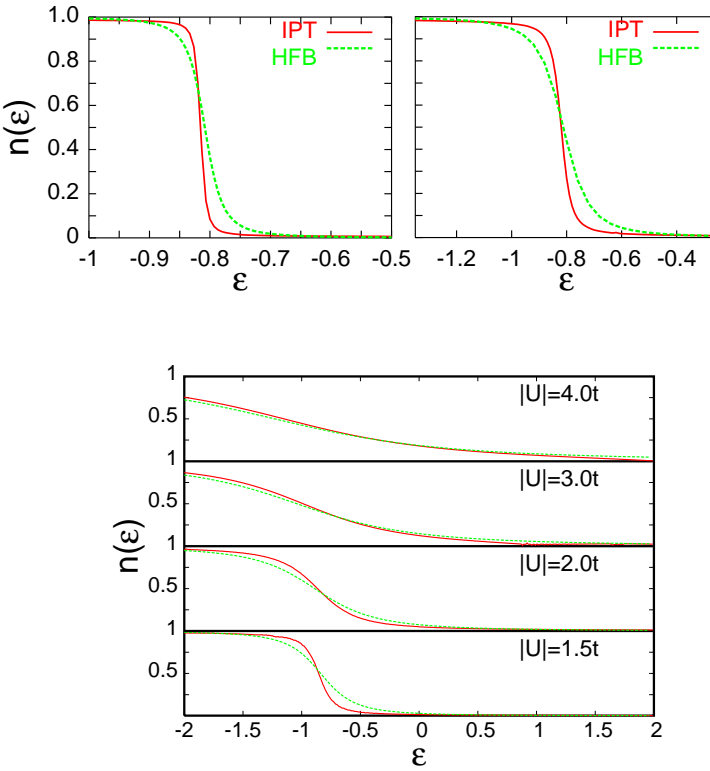


FIG . 9: The occupation probability $n(\epsilon)$ of an energy level for $n = 0.5$, $T = 0$ for various values of $|U|/t$ obtained within IPT (red curve) and HFB approximation (green curve). Top right panel shows $n(\epsilon)$ for $|U|/t = 0.75t$ and top left panel shows $n(\epsilon)$ for $|U|/t = 1.0t$. Note scale over which these are plotted are different. Bottom panel shows $n(\epsilon)$ for $|U|/t = 1.5t, 2.0t, 3.0t$ and $4.0t$ starting from bottom to top.

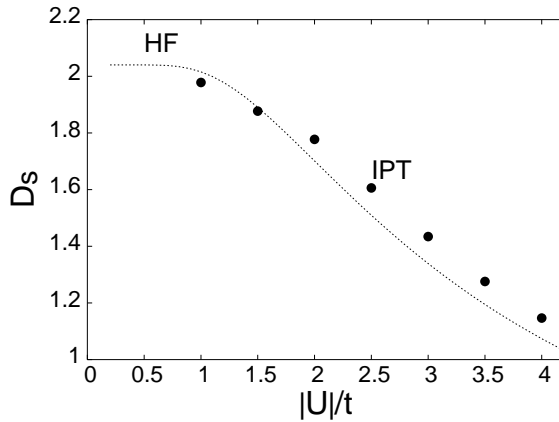


FIG . 10: Upper bound on the superuid stiness D_s for $n = 0.5$, $T = 0$ as a function of the coupling constant $|U|/t$ within IPT (filled circles) and HFB theory (dotted line).

a function of the attractive interaction. We find that it is of order t in weak coupling, but decreases monotonically with $|U|/t$ reaching $t = |U|/t$ in the strong coupling limit, which reflects the increasing effective mass of the hard core lattice bosons in the large $|U|/t$ limit.

6. CONCLUSIONS

In this paper we have studied the crossover from BCS superconductivity to BEC at $T = 0$ in the attractive Hubbard model using dynamical mean field theory (DMFT), implemented using the iterated perturbation theory (IPT) scheme. Our main goal was to explore the DMFT approach in a broken symmetry state, which has received less attention than the paramagnetic phase, within a simple, easily implemented, semi-analytic scheme, and to see how the quantum fluctuations included in this framework modify the Hartree-Fock-Bogoliubov (HFB) mean field results. For the most part we found that HFB is qualitatively correct but overestimates the SC order parameter and energy gap. In the intermediate coupling regime, the quantitative changes can be quite large. The frequency dependent self-energy of DMFT leads to the appearance of incoherent contributions to the single particle spectral function at energies larger than three times the gap, and the consequent reduction in the coherent spectral weight in the Bogoliubov quasiparticle/quasihole poles in the spectrum.

ACKNOWLEDGMENTS

A.G. would like to thank S.R. Hassan and R. Karan for many useful discussions and acknowledge the hospitality of the Department of Physics, IISc., Bangalore, over a period during which a part of this work was done. M.R.'s work at TIFR was supported in part by the Department of Science and Technology under a Swami Jayanti Grant.

APPENDIX A : LARGE ! LIMIT

In this Appendix we will first determine the large $!$ limit of the self energy and then use it to fix the parameter \hat{A} in our IPT ansatz (18). The $! \rightarrow 1$ limit can be obtained by a moment expansion of the Green's function

$$G(!^+) = \frac{1}{!^+} M^{(0)} + \frac{M^{(1)}}{!^+} + \frac{M^{(2)}}{!^2} + \dots ; \quad (43)$$

which follows from the spectral representation

$$G(!^+) = \frac{\int_1^{\infty} G(\epsilon) d\epsilon}{!^+} \quad (44)$$

and the definition of the n^{th} moment of the density of states $M^{(n)} = \int_1^{\infty} G(\epsilon) \epsilon^n d\epsilon$.

To evaluate the moments it is useful to go to a Hamiltonian formulation for single site impurity problem, which requires introducing auxiliary degrees of freedom to describe the 'bath'. For the superconducting phase of the negative U Hubbard model, one possible choice for the

impurity Ham iltonian is :

$$H_{\text{imp}} = \sum_k^X c^\dagger c - \sum_k^X \mu_j n_k + \sum_k^X f_k^\dagger f_k + \sum_k^X V_k c^\dagger f_k + f_k^\dagger c + D \sum_k^X f_k^\dagger f_{k\#}^\dagger + f_{k\#}^\dagger f_k^\dagger \quad (45)$$

which describes the impurity c coupled to superconducting bath of f fermions. Here V_k is the hybridization parameter which allows fermions to hop between the bath and the impurity site and the D term represents s-wave pairing of the f 's.

Using the spectral representation, the moments can be written in terms of commutators ($[;]$) and anticommutators ($\{;g\}$) involving the c 's and the impurity Ham iltonian:

$$\hat{M}^{(0)} = \sum_i^n c^\dagger_i c_i = \quad (46)$$

$$\hat{M}^{(1)} = \sum_i^n [c_i; H_{\text{imp}}] c^\dagger_i \quad (47)$$

and

$$\hat{M}^{(2)} = \sum_i^n [c_i; [H_{\text{imp}}; H_{\text{imp}}]] c^\dagger_i \quad (48)$$

where $; = ";\#$. Explicit evaluation of these commutators leads to the results

$$\hat{M}^{(1)} = (\sum_j^2 \mu_j) \hat{z} + \hat{x} \quad (49)$$

$$\hat{M}^{(2)} = \hat{z}^2 + \frac{(2 \sum_j^2 \mu_j + U^2)n}{2} \hat{z} \quad (50)$$

The Host Green's function \hat{G} is obtained from the impurity Ham iltonian setting $U = 0$, and its large $!$ limit is

$$\hat{G}^{-1}(!^+) = \sum_k^X V_k^2 = !^z \quad (51)$$

Using the Dyson equation, the large $!$ limit of selfenergy is then found to be

$$\hat{\Sigma}(!^+) = \hat{\Sigma}_{\text{HFB}} + \frac{U^2 n (1 - n=2=2)}{!^+} \hat{z} \quad (52)$$

We must now find the large $!$ limit of IPT selfenergy, and compare it with the exact $!$ result (52) derived above. Begin with the diagonal component of $\hat{\Sigma}^{(2)}(!)$ given by

$$\hat{\Sigma}^{(2)}(!^+) = U^2 \sum_{i=1}^Z \sum_{j=1}^Y d_i \frac{g_1(1; 2; 3) N(1; 2; 3)}{w^+} \quad (53)$$

where

$$g_1(1; 2; 3) = \gamma_{11}(1) \gamma_{22}(2) \gamma_{22}(3) - \gamma_{11}(1) \gamma_{22}(2) \gamma_f(3) \quad (54)$$

Here $\gamma_{ii}(!) = 1 = \text{Im } G_{ii}(!^+)$ with $i = 1, 2$ and $\gamma_f(!) = 1 = \text{Im } F_0(!^+)$. In the large $!$ limit it suffices to keep terms up to order $1=!$. We thus get

$$\hat{\Sigma}^{(2)}(!^+) = \frac{1}{!^+} \frac{U^2 n_0}{2} (1 - \frac{n_0}{2}) \quad (55)$$

Next, consider the off-diagonal component of $\hat{\Sigma}^{(2)}(!)$

$$\hat{\Sigma}^{(2)}(!^+) = U^2 \sum_{i=1}^Z \sum_{j=1}^Y d_i \frac{g_2(1; 2; 3) N(1; 2; 3)}{w^+} \quad (56)$$

where

$$g_2(1; 2; 3) = \gamma_f(1) \gamma_f(2) \gamma_f(3) - \gamma_{11}(1) \gamma_f(2) \gamma_{22}(3) \quad (57)$$

It is easy to check that in the large $!$ limit $\hat{\Sigma}^{(2)}$ vanishes up to order $1=!$.

Comparing the large $!$ limits of the IPT ansatz $\hat{\Sigma}_{\text{HFB}} + \hat{A}^{(2)}(!)$ and the exact selfenergy (52), we find

$$\hat{A}^{(2)} = \frac{U^2 n_0}{2} (1 - \frac{n_0}{2}) \hat{z}^2 + \frac{U^2 n}{2} (1 - \frac{n}{2}) \hat{z}^2 \quad (58)$$

APPENDIX B : ATOMIC LIMIT

In this Appendix we first solve the attractive Hubbard model exactly in the atomic limit $t=U=0$ and then show that our IPT ansatz for selfenergy is exact in this limit. In the atomic limit one can drop the hopping term in the Hubbard Ham iltonian (and also the hybridization term in the impurity Ham iltonian) so that

$$H = \sum_j^2 \mu_j n_j = (n_+ + n_-) \quad (59)$$

The various sites decouple and so we have dropped the site label. The four states are $|j\rangle_i; j^\dagger i; j\#i$ and $j^\dagger \#i$ with corresponding energies $0; \pm \mu$ and $\pm \sqrt{2} \mu$.

To study the broken symmetry phase we introduce a pairing field h ,

$$H = \sum_j^2 \mu_j n_j = (n_+ + n_-) - h (c^\dagger c + c^\dagger c) \quad (60)$$

and finally take the $h \rightarrow 0$ limit. The $T=0$ equations for the filling factor and order parameter are given by

$$n = \frac{2}{1 + (h=)^2} \text{ and } = \frac{\mu}{1 + (h=)^2} \quad (61)$$

where $= \sqrt{(2 + \mu)^2 - 4h^2} = 2$ is the lowest eigenvalue of the Ham iltonian. We thus find that

in the $\hbar \rightarrow 0$ limit we get the atom $\hbar \rightarrow 0$ limit solution: $\hat{G}^{-1}(w) = \frac{1}{2} + \frac{1}{w + \frac{1}{2} + \frac{J(J+2)}{w + J(J+2) + 1}}$ for any filling n and $J(J+2) = n(2-n)$.

Now consider the HFB equations in the atom $\hbar \rightarrow 0$ limit at $T = 0$:

$$n = \frac{1}{2} + \frac{1}{w + \frac{J(J+2)}{(w + J(J+2))^2 + 1}} \quad (62)$$

and

$$\frac{1}{J(J+2)} = \frac{1}{w + \frac{J(J+2)}{(w + J(J+2))^2 + 1}} \quad (63)$$

The solution of these self-consistent equations is $\hat{G}^{-1}(w) = \frac{1}{2} + \frac{1}{w + \frac{J(J+2)}{n(2-n)}}$, which shows that HFB theory is exact in the atom $\hbar \rightarrow 0$ limit at zero temperature.

Finally we will show that the second order self-energy vanishes in the atom $\hbar \rightarrow 0$ limit. The Hartree corrected Hartree-Green's function

$$\hat{G}^{-1}(w) = \hat{G}^{-1}(w) + \hat{\Delta}_{\text{HFB}} \quad (64)$$

reduces in the atom $\hbar \rightarrow 0$ limit to

$$\hat{G}^{-1}(w) = w + \hat{\Delta}_0 + \frac{1}{w + \frac{J(J+2)}{n(2-n)}} \quad (65)$$

It can be checked that the full Green's function in the atom $\hbar \rightarrow 0$ limit is identical to this, which means that $\hat{\Delta}_0$ vanishes. Alternatively one can calculate the density of states corresponding to \hat{G}_0 , which are given by

$$\hat{\rho}_1(w) = (1 - n(2-n)) \left(w - \frac{J(J+2)}{n(2-n)} \right) \quad (66)$$

and

$$\hat{\rho}_2(w) = -J(J+2) \left(w - \frac{J(J+2)}{n(2-n)} \right) \quad (67)$$

and substitute these in the expression for the $\hat{\Delta}_0$ and check that all the components of second order self-energy matrix vanish in the atom $\hbar \rightarrow 0$ limit.

[6] C. A. R. Sa de Melo, M. Randeria, and J. R. Engelbrecht, Phys. Rev. Lett. 71, 3202 (1993); J. R. Engelbrecht, M. Randeria, and C. A. R. Sa de Melo, Phys. Rev. B 55, 15,153 (1997).

[7] M. Randeria, N. Trivedi, A. Moreo, and R. T. Scalettar, Phys. Rev. Lett. 69, 2001 (1992).

[8] N. Trivedi and M. Randeria, Phys. Rev. Lett. 75, 312 (1995).

[9] S. Jochim, M. Bartenstein, A. Altmeyer, G. Hänsel, S. Riedl, C. Chin, J. H. Denschlag, and R. Grimm, Science 302, 2101-2103 (2003), M. Bartenstein, A. Altmeyer, S. Riedl, S. Jochim, C. Chin, J. H. Denschlag, and R. Grimm, Phys. Rev. Lett. 92, 120401 (2004) and Phys. Rev. Lett. 92, 203201 (2004), C. A. Regal, M. G. Reiner, and D. S. Jin, Phys. Rev. Lett. 92, 040403 (2004) and condmat/0311172, M. G. Reiner, C. A. Regal, and D. S. Jin, Nature 426, 537 (2003), M. W. Zwierlein, C. A. Stan, C. H. Schunck, S. M. F. Raupach, S. Gupta, Z. Hadzibabic, and W. Ketterle, Phys. Rev. Lett. 91, 250401 (2003), Z. Hadzibabic, S. Gupta, C. A. Stan, C. H. Schunck, M. W. Zwierlein, K. Dieckmann, and W. Ketterle, Phys. Rev. Lett. 91, 160401 (2003), S. Gupta, Z. Hadzibabic, M. W. Zwierlein, C. A. Stan, K. Dieckmann, C. H. Schunck, E. G. M. van Kempen, B. J. Verhaar, and W. Ketterle, Science 300, 1723-1726 (2003), M. W. Zwierlein, C. A. Stan, C. H. Schunck, S. M. F. Raupach, A. J. Kerman, and W. Ketterle, Phys. Rev. Lett. 92, 120403 (2004).

[10] A. Georges, G. Kotliar, W. Krauth, and M. J. Rozenberg, Rev. Mod. Phys. 68, 13 (1996).

[11] T. P. Ruschke, M. Jarrell, and J. K. Freericks, Adv. Phys. 44, 187 (1995).

[12] M. Keller, W. Metzner, and U. Schollwock, Phys. Rev. B, 60, 3499 (1999), Phys. Rev. Lett. 86, 4612 (2001) and condmat/0109343, M. Capone, C. Castellani, and M. Grilli, Phys. Rev. Lett. 88, 126403 (2002).

[13] L. Belkhir and M. Randeria, Phys. Rev. B 49, 6829 (1994).

[14] Modern Quantum Mechanics by J. J. Sakurai chapter 7 eds. (Pearson Education, 1999).

[15] H. Kajueter and G. Kotliar, Phys. Rev. Lett. 77, 131 (1996).

[16] M. Jarrell, Phys. Rev. Lett. 69, 168 (1992), M. J. Rozenberg, X. Y. Zhang, and G. Kotliar, Phys. Rev. Lett. 69, 1236 (1992), A. Georges and W. Krauth, Phys. Rev. Lett. 69, 1240 (1992).

[17] M. Cararel and W. Krauth, Phys. Rev. Lett. 72, 1545 (1994), M. J. Rozenberg, G. Moeller, and G. Kotliar, Rev. Mod. Phys. Lett. 8, 535 (1994), Q. Si, M. J. Rozenberg, G. Kotliar and A. E. Ruckenstein, Phys. Rev. Lett. 72, 2761 (1994).

[18] K. G. Wilson, Rev. Mod. Phys. 47, 773 (1975), H. R. Krishnamurthy, J. W. Wilkins, and K. G. Wilson, Phys. Rev. B 21, 1003 (1980), O. Sakai, Y. Kuroki, Solid State Commun. 89, 307 (1994), R. Bulla, A. C. Hewson, and Th. Ruschke, J. Phys. Condens. Matter 10, 8365 (1998), R. Bulla, T. A. Costi, and D. Vollhardt, Phys. Rev. B 64, 045103 (2001), D. M. Eyer, A. C. Hewson, and R. Bulla, Phys. Rev. Lett. 89, 196401 (2002).

[19] D. E. Logan, M. P. Eastwood, and M. A. Tusch, J. Phys. Condens. Matter 10, 2673 (1998), N. L. D. Dicks and D. E. Logan, J. Phys. Condens. Matter 13, 4505 (2001), D. E. Logan and N. L. D. Dicks, J. Phys. Condens. Matter 13, 9713 (2001), D. E. Logan and N. L. D. Dicks, J. Phys.

[1] D. M. Eagles, Phys. Rev. 186, 456 (1969).

[2] A. J. Leggett in Modern Trends in the Theory of Condensed Matter, A. P. Pekalski and R. Przystawa, eds. (Springer-Verlag, Berlin, 1980); and J. Phys. (Paris) Colloq. 41, C7-19 (1980).

[3] P. Nozieres and S. Schmitt-Rink, J. Low Temp. Phys. 59, 195 (1985).

[4] For a review, see M. Randeria in *Bose-Einstein Condensation*, edited by A. Griffin, D. Snoke, and S. Stringari, (Cambridge University Press, Cambridge, England, 1994).

[5] M. Randeria, J. M. Duan, and L. Y. Shieh, Phys. Rev. Lett. 62, 981 (1989) and Phys. Rev. B, 41, 327 (1990).

Condens. Matter 14, 3605 (2002), V. E. Smith, D. E. Logan, and H. R. Krishnamurthy, condmat/0303229, N. S. Vidyadhara, V. E. Smith, D. E. Logan, and H. R. Krishnamurthy, condmat/0307462.

[20] Note that we do not impose the Luttinger Integral Theorem (also referred to as the Luttinger sum rule). While its importance is of importance in metallic systems to ensure Fermi liquid properties [10, 15], we believe that its importance is not as crucial in gapped systems such as the ones under discussion.

[21] We note that in the presence of the IPT contributions to the selfenergy, the values of and , obtained from eqs. (21,20), are different from the values that arise in pure HFB .

[22] Numerical Recipes in Fortran by W. H. Press, S. A. Teukolsky, W. T. Vetterling, and B. P. Flannery page 382, chapter 9 eds. (Cambridge University Press, 1993).

[23] D. J. Scalapino, S. R. White, and S. Zhang, Phys. Rev. B, 47, 7995 (1993).

[24] A. Parameswari, N. Trivedi, and M. Randeria, Phys. Rev. B 57, 11639 (1998).